

Journal of Biomedical Optics

SPIEDigitalLibrary.org/jbo

Evaluation of parameters influencing the molecular delivery by biodegradable microsphere-mediated perforation using femtosecond laser

Tatsuki Mitsuhashi
Mitsuhiro Terakawa

Evaluation of parameters influencing the molecular delivery by biodegradable microsphere-mediated perforation using femtosecond laser

Tatsuki Mitsuhashi and Mitsuhiro Terakawa*

Keio University, School of Integrated Design Engineering, Department of Electronics and Electrical Engineering, 3-14-1 Hiyoshi, Kohoku-ku, Yokohama, Kanagawa 223-8522, Japan

Abstract. The parameters critically influencing the delivery rate on the biodegradable microsphere-mediated femtosecond (fs) laser perforation are investigated in detail with the aim of developing efficient molecular delivery. Cell membrane was perforated by the irradiation of weakly focused fs laser pulses to the spherical polylactic acid microspheres conjugated to the cell membrane. The delivery of fluorescein isothiocyanate-dextran and fluorescent silica particles to A431 cells is investigated in detail. The increase in the number of irradiated laser pulses had resulted in the increase of delivery rate. The delivery rate depends on the size and functionalization of fluorescent silica particles in which silica particles of 100 nm in diameter were able to be delivered into 20% of the irradiated cells, suggesting that the pore sizes are large enough for the delivery of therapeutic agents into cells. These findings contribute to the development of an efficient and safe phototherapy and drug delivery. © 2014 Society of Photo-Optical Instrumentation Engineers (SPIE) [DOI: [10.1117/1.JBO.19.1.015003](https://doi.org/10.1117/1.JBO.19.1.015003)]

Keywords: femtosecond laser; cell perforation; transfection; drug delivery; biodegradable polymer; nanomedicine.

Paper 130614R received Aug. 22, 2013; revised manuscript received Nov. 28, 2013; accepted for publication Dec. 3, 2013; published online Jan. 3, 2014.

1 Introduction

In recent years, applications of nano- and micro-particles in biomedicine are expanding. Particles of different materials and sizes have been used to suit a variety of purposes such as diagnosis,¹ cancer therapy,² and drug delivery.³ The methods of utilizing the interaction of a laser and such particles have a precise time- and spatial-controllability and are easy to be applied to catheter-based therapy by using an optical fiber. Several studies have reported the enhancement of cell membrane permeability by utilizing the absorption of laser energy by particles such as carbon black particles and metallic particles. In the method of using a carbon black particle, the enhancement of cell membrane permeability has been demonstrated by the irradiation of a femtosecond (fs) laser, in which the carbon-steam reaction followed by the generation of an acoustic shockwave may have contributed to the enhancement.⁴ As for the method of using a gold particle, the interaction of gold particles and nanosecond or fs laser pulses has resulted in the enhancement of cell membrane permeability. When irradiating nanosecond laser pulses, temperature rise of gold particles and/or generation of plasma due to the highly enhanced optical near field could result in the formation of a cavitation bubble followed by the generation of shockwave pressure.⁵⁻⁷ In the case of using fs laser pulses, the optical near field around gold particles could yield ablation of cell membrane and bubble formation followed by shockwave pressure generation.^{8,9} The interaction could be confined in a limited space during the perforation. Baumgart et al. calculated that the spheroidal bubble generated around the 100-nm diameter gold particle by fs laser irradiation (fluence 200 mJ/cm², 45 fs pulse width, and 800-nm wavelength) has a maximal

average diameter of around 1.2 μm . The peak pressure of the generated shockwave reaches 80 GPa at the surface of the gold particle, and the maximum pressure drops below 1 GPa as near as 200 nm from the nano particle (NP) center.⁸ The size of a pore formed on a cell membrane is one of the critical conditions on the laser-based cell perforation. Bhattacharyya et al. estimated the size of a pore formed on a cell membrane to be smaller than 20 nm in diameter when nanosecond laser pulses were irradiated to gold particles of 54 nm in diameter on the cell membrane.¹⁰ Several studies on cell selective perforation that utilize gold particles conjugated to the cell membrane by an antigen-antibody reaction have been reported,^{11,12} although the cytotoxicity of the gold particles is still under discussion.^{13,14} As an alternative method, cell membrane perforation using biodegradable microspheres has the potential to achieve low-cytotoxic drug delivery.^{15,16} We have demonstrated the cell membrane perforation by the irradiation of a single shot of weakly focused fs laser to the transparent dielectric microspheres selectively conjugated to the cell membrane.^{17,18} When the laser is irradiated, an enhanced optical field is generated under the microsphere in the vicinity of the cell membrane, which could lead to the nonlinear interaction.

On the study of drug delivery into cells, revealing the parameters critically influencing the delivery realizes a highly efficient delivery as well as the elucidation of the underlying mechanism. For example, it has been demonstrated that the cell membrane fluidity influences cell membrane permeability on the basis of the experiments of changing the ambient temperature when applying electroporation.¹⁹ Molecules of different sizes were used to study the mechanism of ultrasound-mediated drug delivery.²⁰

*Address all correspondence to: Mitsuhiro Terakawa, E-mail: terakawa@elec.keio.ac.jp

In the present study, we attempted to identify the parameters critically influencing the delivery rate on the biodegradable microsphere-mediated fs laser perforation. The influences of the ambient temperature, the number of irradiated laser pulses, the delivered molecules' size, and the charge of the molecule on the delivery rate were investigated. The results of changing these parameters would depend little on the cell type and could contribute to the fundamental understanding of the mechanism.

2 Materials and Methods

2.1 Cell Culture

Human epithelial carcinoma cells (A431 cells) were cultured in Dulbecco's modified Eagle's medium supplemented with 10% fetal bovine serum under a humidified atmosphere of 95% air and 5% CO₂ at 37°C. The cells were harvested and seeded as a monolayer in glass-bottom culture dishes for the experiments.

2.2 Cell Membrane Perforation

Spherical protein A bound polylactic acid (PLA) microspheres of 2 μm in diameter were mixed with anti-epidermal growth factor receptor mouse monoclonal antibody (Thermo Fisher Scientific, Fremont, California). The mixture was stirred for 25 min at room temperature, and then the unbound antibody was removed by centrifugation for 10 min at 10,000 rpm. The bound PLA microspheres were resuspended in phosphate-buffered saline (PBS) and added to A431 cells. The cells were incubated for 40 min under a humidified atmosphere of 95% air and 5% CO₂ at 37°C and washed three times with PBS in order to remove the unconjugated microspheres. A Ti:sapphire chirped pulse amplification laser system (Libra, Coherent, Santa Clara, California), which generates 80-fs laser pulses at an 800-nm central wavelength, was used in the experiments. The laser beam was weakly focused by using a plano-convex lens ($f = 200$ mm) to a laser spot size of 300 μm which was determined by full-width-at-half-maximum (FWHM) of the peak intensity of the Gaussian beam. Many cells can be treated simultaneously because a number of cells were inside the laser spot. The cells were irradiated by a single or multiple shot(s) of polarized (linearly or circularly) laser pulse from the top side of the cells. The PLA microsphere works as a microlens, and the optical intensity was enhanced by 9.7 at 870 nm under the PLA microsphere calculated by the three-dimensional finite-difference time-domain method. The optical intensity distribution under the PLA microsphere is described in our previous paper.¹⁸ The fluorescein isothiocyanate (FITC)-dextran solution or the green fluorescent silica particle suspension was added to the cells just before the laser irradiation. Two minutes after the irradiation, the cells were washed three times with PBS. Fluorescent molecules delivered into the cells were observed by using a fluorescence microscope (Eclipse Ti-E, Nikon, Tokyo, Japan). The delivery rate was evaluated by counting the number of cells inside the laser spot, and it was calculated by the number of cells inside the laser spot showing fluorescence divided by the number of cells inside the laser spot. Only the cells attached to the dish were counted. All values in the figures were expressed as means ± standard deviation.

2.3 Dependence of Delivery Rate on the Ambient Temperature

Simultaneous application of mild heat may influence cell membrane permeabilization when a physical method for drug delivery was applied.¹⁹ The effect of cell membrane fluidity on the delivery rate was evaluated by changing the ambient temperature of the cells.

After the removal of the unconjugated PLA microspheres from the cells, the culture dish was placed on a thermo plate (Tokai Hit Company, Shizuoka, Japan). The temperature of the medium was controlled by the heating stage and monitored by a thermocouple thermometer. During the perforation experiment, the ambient temperature was kept at 23, 37, or 40.5°C. The FITC-dextran (4 kDa and 2 MDa; Sigma, St. Louis, Missouri) was used to evaluate the efficiency of delivery. The FITC-dextran solution (0.5 mM for 4 kDa and 0.001 mM for 2 MDa) was added to the cells just before the linearly polarized fs laser irradiation. The cells were irradiated by a single shot of fs laser pulse.

2.4 Dependence of Delivery Rate on the Number of Irradiated Laser Pulses

The interaction between a fs laser pulse and cell membrane is governed by the peak laser intensity. Although high peak intensity is necessary for nonlinear optical interactions, excess laser intensity may lead to cell damage. To realize a cell membrane perforation with lower laser intensity, we have conducted an experiment using multiple laser pulses.

The FITC-dextran (4 kDa and 2 MDa) and the green fluorescent silica particles (plain or functionalized, 100 nm in diameter) were used to evaluate the efficiency of delivery. They were added to the cells at 23°C just before the circularly polarized fs laser irradiation (1, 2, 5, and 10 pulses). The repetition rate of the laser system was 1 kHz, and the number of shots was controlled by using a digital delay generator (DG535, Stanford Research Systems, Sunnyvale, California) to control the Pockels cell inside the laser system. The laser fluence was 1.06 or 0.53 J/cm² at which the corresponding peak laser intensity under the microsphere is estimated to be 1.29×10^{14} or 6.43×10^{13} W/cm², respectively.¹⁸

2.5 Dependence of Delivery Rate on the Delivered Particle Size

Different sizes of spherical particles were delivered into the cells to investigate and discuss the size of the pores formed on the cell membrane.

The green fluorescent silica particles (diameters of 30, 50, 70, 100, 200, and 500 nm) (sicstar, Micromod, Rostock-Warnemünde, Germany) were used to evaluate the size-dependent efficiency of delivery. After the removal of the unconjugated PLA microspheres, the silica particle suspension (2.5 mg/ml) was added to the cells at 23°C just before the circularly polarized fs laser irradiation. The laser fluence was 1.06 J/cm².

2.6 Dependence of Delivery Rate on the Charge of Delivered Particles

Since the cell membrane is negatively charged, the charge of molecules could influence the delivery rate when using physical methods to enhance the cell membrane permeability.^{21,22} The

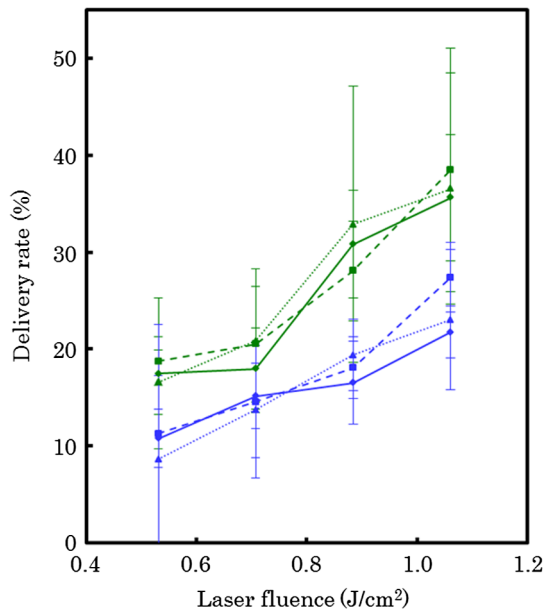


Fig. 1 Dependence of delivery rate on cell's ambient temperature at different laser fluences. Delivery rate was evaluated by using fluorescein isothiocyanate (FITC)-dextran of 4 kDa (green) and 2 MDa (blue) at the ambient temperature of 23°C (diamond), 37°C (square), and 40.5°C (triangle).

charged silica particles were delivered into the cells to investigate the influence of the charge on the delivery rate by the biodegradable microsphere-mediated perforation using a fs laser.

The green fluorescent silica particles of 100 nm in diameter with functionalized surface were used to evaluate the efficiency of delivery. Aminated or carboxylated particles (sicastar, Micromod) were chosen as they are positively and negatively charged, respectively. After the removal of the unconjugated

PLA microspheres from the cells, the silica particle suspension (2.5 mg/ml) was added to the cells at 23°C just before the circularly polarized fs laser irradiation. The laser fluence was 1.06 J/cm².

3 Results

3.1 Ambient Temperature Dependence

Figure 1 shows the dependence of the delivery rate of FITC-dextran on the ambient temperature of the cells. Delivery rates with both 4 kDa and 2 MDa FITC-dextran had no statistically significant difference depending on the temperature. In this experiment, the cells were heated to the specified temperatures before and during the laser irradiation, in which the total heating time was less than 3 min. The 4-kDa FITC-dextran was delivered with higher rates compared with the FITC-dextran of 2 MDa. This result is probably related to the size of the pores formed on the cell membrane, which allowed the smaller FITC-dextran to be delivered and made it difficult for larger FITC-dextran to cross the pores. We have not investigated the effect of the temporal heating dose in this study, but it would affect the survival rate of the cells if the heating time is long. Figure 1 also shows the dependence of the delivery rate on the laser fluence. The delivery rate increased with increasing laser fluence. The peak intensity under the sphere is determined by multiplying the incident laser intensity by the enhancement factor under the PLA sphere. Thus, the figure also indirectly shows the effect of the enhancement factor.

3.2 Dependence the Delivery Rate of FITC-Dextran on the Number of Irradiated Pulses

Figure 2 shows the phase-contrast and fluorescence images of the cells after the laser irradiation at the laser fluence of 1.06 J/cm² with different numbers of pulses. Cell detachment

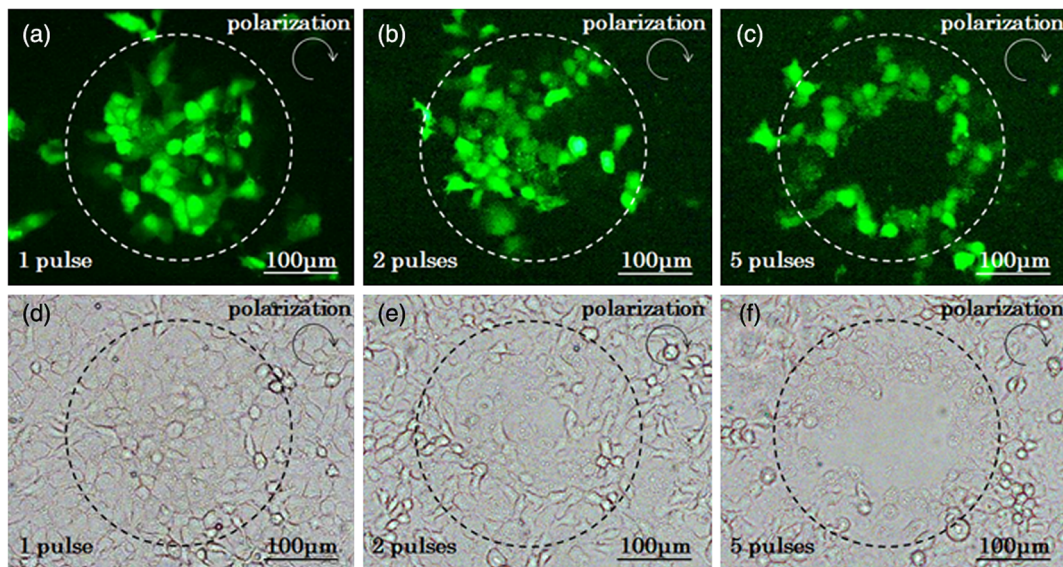


Fig. 2 (a–c) Fluorescence and (d–f) phase contrast images of A431 cells perforated by using antibody-conjugated poly(lactic acid) (PLA) microspheres irradiated by femtosecond (fs) laser pulse(s) in the presence of 4-kDa FITC-dextran. The number of irradiated laser pulses were 1 (a, d), 2 (b, e), and 5 (c, f). The irradiated laser fluence was 1.06 J/cm² at the ambient temperature of 23°C. Dashed circles (300-µm diameter) indicate the laser-irradiated area.

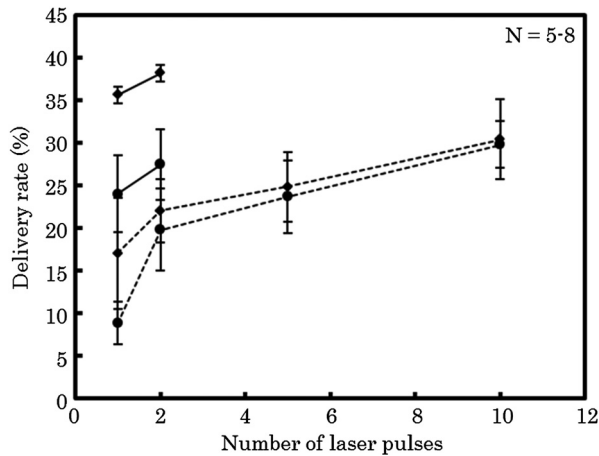


Fig. 3 Dependence of delivery rate on the number of laser pulses. Delivery rate was evaluated by FITC-dextran of 4 kDa (diamond) and 2 MDa (circle). The irradiated laser fluence was 1.06 J/cm^2 (solid line) and 0.53 J/cm^2 (dashed line). The evaluation of the delivery rate was difficult for more than 5 pulses at 1.06 J/cm^2 or 50 pulses at 0.53 J/cm^2 , since the cell detachment was observed in the center of the laser-irradiated area.

can be observed in the center of the laser irradiated area when irradiating five or more pulses at 1.06 J/cm^2 , which resulted in difficulties of the evaluation of the delivery rate. We considered that the detached cells are dead and that the laser fluence, which leads to the detachment of the cells, should not be applied to drug delivery system (DDS) applications including *in vivo* therapy. Several cells near the irradiated area showed fluorescence which is probably due to the low-laser intensity outside the laser spot of the Gaussian beam profile. Figure 3 shows the delivery rate of FITC-dextran with different numbers of pulses at two different laser fluences. The delivery rates for control experiments, i.e., delivery rates without laser irradiation, were $0.5 \pm 0.5\%$ and $0.3 \pm 0.6\%$ for FITC-dextran of 4 kDa and 2 MDa, respectively. The delivery rate increased with the increasing number of laser pulses. Cells were attached to the bottom of the dish after the irradiation of 10 pulses at 0.53 J/cm^2 .

3.3 Investigation of the Size of Pores on Cell Membrane

We investigated the size of the pores formed on the cell membrane by using different sizes of green fluorescent silica particles. An optical intensity distribution under a PLA microsphere varies depending on the polarization direction of the irradiated laser. In the case of silica substrate surface ablation, the hole fabricated by using dielectric particles had a different shape depending on the polarization of the incident laser.²³ As for the perforation of cell membrane, the delivery rate could be influenced by the polarization direction of the irradiated laser (especially for the delivery of silica particles with large diameter) which would form different shapes of pores. Therefore, we have investigated the dependence of the delivery rate on the laser polarization. Figure 4 shows the calculated optical intensity distributions under the PLA microsphere of $2\text{-}\mu\text{m}$ diameter in water irradiated by a plain 800-nm light. The optical intensity distribution of 5-nm under the microsphere and 940-nm under the microsphere, where the peak intensity is obtained, was elliptical (the long axis in the polarized direction) with

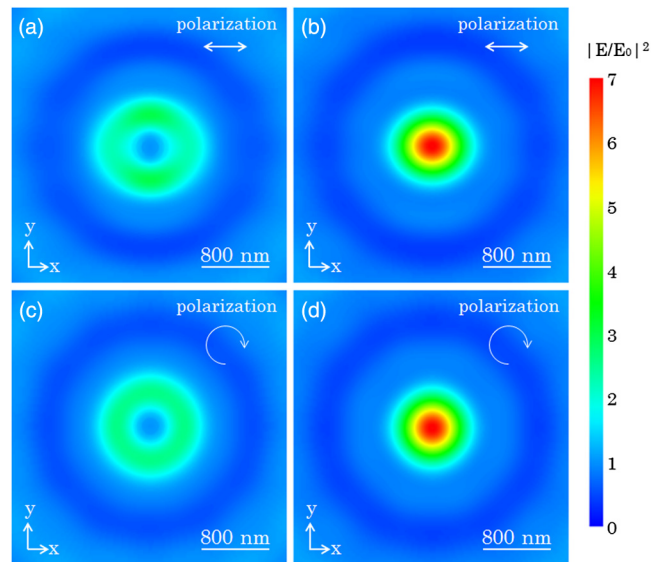


Fig. 4 Optical intensity distributions on the xy plane (a, c) 5-nm under the PLA microsphere and (b, d) on the peak intensity (940-nm under the microsphere) simulated by the three-dimensional finite-difference time-domain method. A plane wave is irradiated to the microsphere with the wave vector in the z -direction. The incident wave of 800 nm in wavelength is polarized (a, b) linearly and (c, d) circularly.

the x -axis linear polarization [Figs. 4(a) and 4(b)] and circular with the circular polarization [Figs. 4(c) and 4(d)]. The FWHM of the optical distribution for linear polarization 940-nm under the microsphere was 610 nm along x -axis and 530 nm along y -axis, whereas that for circular polarization 940-nm under the microsphere was 570 nm along both x - and y -axes. However, as shown in Fig. 5, no significant difference in the delivery rate of FITC-dextran was obtained between circular and linear polarizations. Hereafter, we describe results by using circularly polarized laser. Figure 6 shows the dependence of delivery rate on the size of the delivering particles. The green fluorescent silica particles of different sizes were used in this study. Although the delivery rate had decreased as the diameters of the particles increased, silica particles with 100-nm diameter were able to be delivered into more than 20% of the cells in the laser-irradiated area.

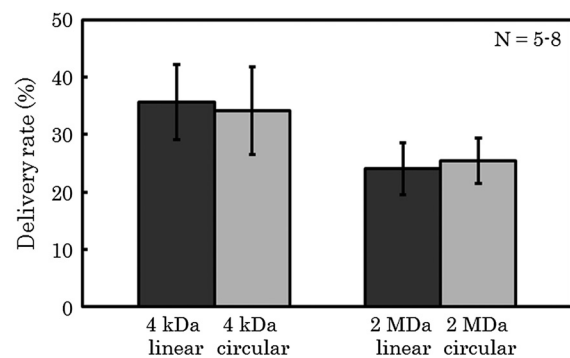


Fig. 5 Dependence of delivery rate on the laser polarization. The delivery rate was evaluated by FITC-dextran of 4 kDa and 2 MDa. A single shot of linearly or circularly polarized 80-fs laser pulse was irradiated at the laser fluence of 1.06 J/cm^2 at the ambient temperature of 23°C .

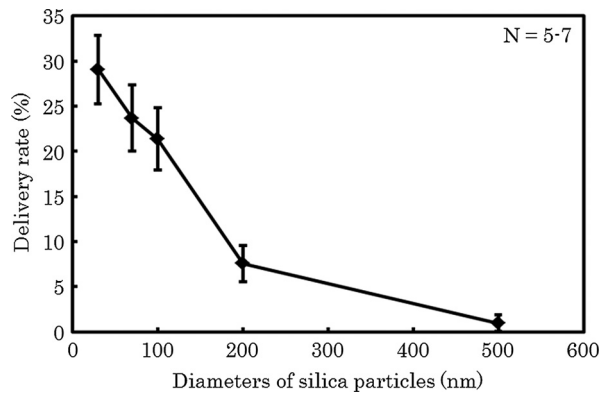


Fig. 6 Dependence of delivery rate on the diameters of silica particles. The delivery rate was evaluated by green fluorescent silica particles of the diameters of 30, 50, 70, 100, 200, and 500 nm. A single shot of 80-fs laser pulse was irradiated at the laser fluence of 1.06 J/cm^2 at the ambient temperature of 23°C .

3.4 Delivery of Functionalized Green Fluorescent Silica Particles

Figure 7 shows the delivery rate of functionalized green fluorescent silica particles. The positively charged particles were able to be delivered at a higher rate than the particles without surface functionalization.

3.5 Dependence of the Delivery Rate of Green Fluorescent Silica Particles on the Number of Irradiated Pulses

Figure 8 shows the delivery rate of functionalized green fluorescent silica particles with different number of pulses at the laser fluence of 0.53 J/cm^2 . The delivery rate increased with the increasing number of irradiated pulses and was saturated at five or more pulses.

4 Discussion

Several studies have reported the difference in delivery rate of molecules into the cells by changing the temperature around the

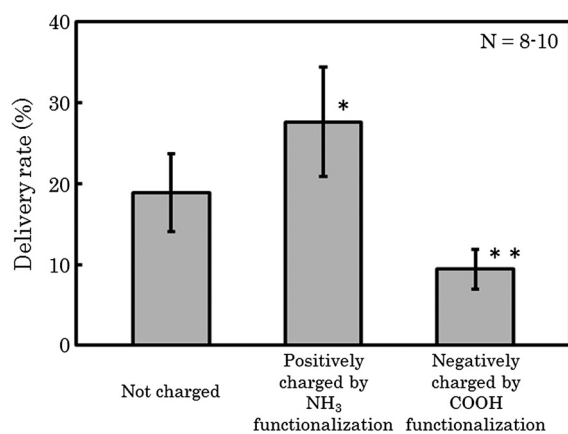


Fig. 7 Dependence of delivery rate on the surface functionalization of green fluorescent silica particles. The delivery rate was evaluated by the plain (not charged), aminated, or carboxylated green fluorescent silica particles with diameters of 100 nm. A single shot of 80-fs laser pulse was irradiated at the laser fluence of 1.06 J/cm^2 . * $p < 0.05$ and ** $p < 0.01$ versus "not charged."

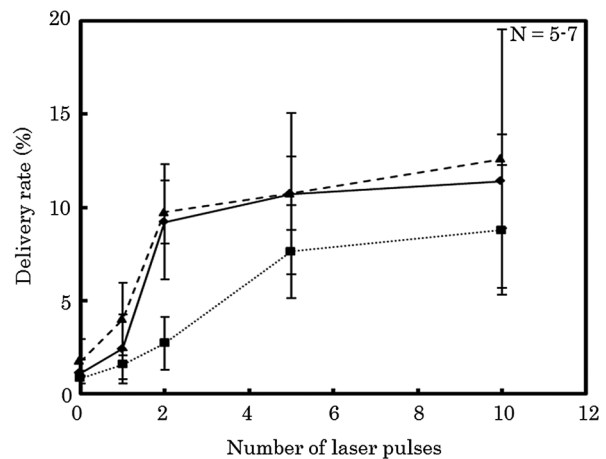


Fig. 8 Dependence of delivery rate of green fluorescent silica particles on the number of laser pulses. The delivery rate was evaluated by plain (diamond), aminated (triangle), and carboxylated (square) green fluorescent silica particles with diameters of 100 nm. The laser fluence was 0.53 J/cm^2 .

cells. It is considered that not only the increase in cell membrane fluidity,^{19,24,25} but also the increase in the diffusion rate of plasmid DNA²⁶ by the temperature rise contribute to the improvement of delivery rate. For the method using gold nanoparticles and picosecond laser for cell membrane perforation, the delivery rate did not depend on the cell membrane fluidity.²⁷ In our study, an experiment was carried out at three different temperatures, but little difference was observed in delivery rate as shown in Fig. 1. The diffusion rate of the FITC-dextran and the fluidity of the cell membrane were probably changed by the temperature, but the temperature is not the influencing parameter on the delivery rate in the biodegradable microsphere-mediated cell perforation.

Several studies have reported that the number of laser pulses affect the delivery rate on the laser-based perforation. When irradiating a focused laser directly to the cell membrane, the increase in the number of pulses improves the delivery rate.²⁸ In the case of using a nanosecond laser with gold particles conjugated to the cell membrane, the delivery was reported to be saturated or decreased for more than five pulses, probably due to the melting and/or fragmentation of the particles.^{12,29} If the laser fluence is under the threshold of melting or fragmentation of the particles, the delivery rate could continue to increase even after irradiating with 800 pulses.¹⁰ As shown in Fig. 8, when delivering silica particles of 100 nm in diameter with multiple pulses, the delivery rate was saturated when irradiating five or more pulses. In addition to the possibility of fragmentation of the PLA microspheres, microspheres were possibly unconjugated from the cell membrane, and resulted in the less interaction between the enhanced optical field and the cell membrane.

By investigating the size of the molecules that can be delivered into cells, we can discuss the size of the pores formed on the cell membrane. In the method of using ultrasound, a large number of pores in the sizes ranging from 20 to 100 nm were observed, which resulted in the delivery of 10 kDa to 2 MDa FITC-dextran.²⁰ The different sizes of latex particles³⁰ and quantum dots¹⁰ were used for the estimation of the pore sizes. Recently, therapeutic proteins of 15 to 150 kDa have been delivered to cells by using electroporation.^{31,32} With the conditions we used in the present study, FITC-dextran of 4 kDa and

2 MDa (1.4 and 27 nm in Stokes' radius, respectively) and silica particles of 100 nm in diameter have been delivered. The result indicated that the pore sizes are large enough for the delivery of therapeutic agents into the cells.

The complex composed of positively charged cationized gelatin and plasmid DNA was used for transfection, a delivery of nucleic acid into the cells, under ultrasound irradiation.^{21,22} The positively charged complex is considered to be adhered to the negatively charged cell membrane, and then they may be uptaken into cells. With a subsequent irradiation of ultrasound, cells exhibited a significantly enhanced luciferase activity in contrast to the cationized gelatin alone with or without ultrasound and ultrasound irradiation alone. For the method of using gold nanoparticles and picosecond laser for cell membrane perforation, FITC-dextran with a larger molecular weight had shown much lower fluorescence than FITC-dextran with a smaller molecular weight, which could be due to the increase in the charge.²⁷ In our method, an improvement in delivery rate was realized by using positively charged silica particles. The positively charged particles were able to be delivered with a higher rate than the particles without surface functionalization. Since the particles were added to the cells just before the laser irradiation and the time until they were washed out by PBS was approximately 5 min, it is highly probable that there was little uptake of silica particles by the cells before laser irradiation. Therefore, the higher concentration of positively charged silica particles near the pores contributed to the improvement of the delivery rate.

The delivery rate shown in this study was not as high as that of other methods after lasting improvements.^{9,11} Further improvement of the delivery rate would probably be achieved by optimizing the types of antibody and the time for antigen-antibody reaction depending on cell types which would increase the number of PLA spheres conjugated to the cell membrane.

5 Conclusion

In this study, parameters critically influencing the delivery rate on the biodegradable microsphere-mediated fs laser perforation were investigated. Irradiation of multiple pulses had improved the efficiency even at low-laser fluence. The delivery rate depends on the particles' size. Silica particles of 100 nm in diameter were able to be delivered into 20% of the irradiated cells, suggesting that the pore sizes are large enough for the delivery of therapeutic agents into the cells. The particles' charge influenced the delivery rate, and a more efficient delivery was realized by using the positively charged particles. These findings contribute to the development of an efficient and safe phototherapy and drug delivery.

Acknowledgments

This work was supported in part by JSPS KAKENHI Grant No. 23680058 [Grant-in-Aid for Young Scientists (A)].

References

1. Y.-H. Wang et al., "Photoacoustic/ultrasound dual-modality contrast agent and its application to thermotherapy," *J. Biomed. Opt.* **17**(4), 045001 (2012).
2. L. Gu et al., "Magnetic-field-assisted photothermal therapy of cancer cells using Fe-doped carbon nanoparticles," *J. Biomed. Opt.* **17**(1), 018003 (2012).
3. Y. Jia et al., "Co-encapsulation of magnetic Fe₃O₄ nanoparticles and doxorubicin into biodegradable PLGA nanocarriers for intratumoral drug delivery," *Int. J. Nanomed.* **7**, 1697–1708 (2012).
4. P. Chakravarty et al., "Delivery of molecules into cells using carbon nanoparticles activated by femtosecond laser pulses," *Nat. Nanotechnol.* **5**(8), 607–611 (2010).
5. C. M. Pitsillides et al., "Selective cell targeting with light-absorbing microparticles and nanoparticles," *Biophys. J.* **84**(6), 4023–4032 (2003).
6. B. St-Louis Lalonde et al., "Visible and near infrared resonance plasmonic enhanced nanosecond laser optoporation of cancer cells," *Biomed. Opt. Express* **4**(4), 490–499 (2013).
7. S. Peeters et al., "Mechanisms of nanoparticle-mediated photomechanical cell damage," *Biomed. Opt. Express* **3**(3), 435–446 (2012).
8. E. Boulais, R. Lachaine, and M. Meunier, "Plasma mediated off-resonance plasmonic enhanced ultrafast laser-induced nanocavitation," *Nano Lett.* **12**(9), 4763–4769 (2012).
9. J. Baumgart et al., "Off-resonance plasmonic enhanced femtosecond laser optoporation and transfection of cancer cells," *Biomaterials* **33**(7), 2345–2350 (2012).
10. K. Bhattacharyya, S. Mehta, and J. Viatore, "Optically absorbing nanoparticle mediated cell membrane permeabilization," *Opt. Lett.* **37**(21), 4474–4476 (2012).
11. E. Y. Lukianova-Hleb et al., "Cell-specific transmembrane injection of molecular cargo with gold nanoparticle-generated transient plasmonic nanobubbles," *Biomaterials* **33**(21), 5441–5450 (2012).
12. C. Yao et al., "Elevation of plasma membrane permeability by laser irradiation of selectively bound nanoparticles," *J. Biomed. Opt.* **10**(6), 064012 (2005).
13. Y. Pan et al., "Size-dependent cytotoxicity of gold nanoparticles," *Small* **3**(11), 1941–1949 (2007).
14. S. Abdelhamid et al., "Laser-induced modifications of gold nanoparticles and their cytotoxic effect," *J. Biomed. Opt.* **17**(6), 068001 (2012).
15. J. Nicolas et al., "Design, functionalization strategies and biomedical applications of targeted biodegradable/biocompatible polymer-based nanocarriers for drug delivery," *Chem. Soc. Rev.* **42**(3), 1147–1235 (2013).
16. B. D. Ulery, L. S. Nair, and C. T. Laurencin, "Biomedical applications of biodegradable polymers," *J. Polym. Sci., Part B: Polym. Phys.* **49**(12), 832–864 (2011).
17. M. Terakawa and Y. Tanaka, "Dielectric microsphere mediated transfection using a femtosecond laser," *Opt. Lett.* **36**(15), 2877–2879 (2011).
18. M. Terakawa, Y. Tsunoi, and T. Mitsuhashi, "In vitro perforation of human epithelial carcinoma cell with antibody-conjugated biodegradable microspheres illuminated by a single 80 femtosecond near-infrared laser pulse," *Int. J. Nanomed.* **7**, 2653–2660 (2012).
19. M. Kandušer, M. Šentjurc, and D. Miklavčič, "The temperature effect during pulse application on cell membrane fluidity and permeabilization," *Bioelectrochemistry* **74**(1), 52–57 (2008).
20. R. Karshafian et al., "Ultrasound-induced uptake of different size markers in mammalian cells," in *IEEE Ultrasonics Symposium*, Vol. 1, pp. 1–16, IEEE (2005).
21. H. Hosseinkhani et al., "In vitro transfection of plasmid DNA by amine derivatives of gelatin accompanied with ultrasound irradiation," *Pharm. Res.* **19**(10), 1471–1479 (2002).
22. H. Hosseinkhani et al., "Ultrasound enhancement of in vitro transfection of plasmid DNA by a cationized gelatin," *J. Drug Targeting* **10**(3), 193–204 (2002).
23. T. Sakai, N. Nedyalkov, and M. Obara, "Friction characteristics of sub-micrometre-structured surfaces fabricated by particle-assisted near-field enhancement with femtosecond laser," *J. Phys. D* **40**(23), 7485–7491 (2007).
24. M. Terakawa et al., "Gene transfer into mammalian cells by use of a nanosecond pulsed laser-induced stress wave," *Opt. Lett.* **29**(11), 1227–1229 (2004).
25. M. Terakawa et al., "In vitro gene transfer to mammalian cells by the use of laser-induced stress waves: effects of stress wave parameters, ambient temperature, and cell type," *J. Biomed. Opt.* **11**(1), 014026 (2006).
26. V. G. Zarnitsyn and M. R. Prausnitz, "Physical parameters influencing optimization of ultrasound-mediated DNA transfection," *Ultrasound Med. Biol.* **30**(4), 527–538 (2004).
27. S. Kalies et al., "Enhancement of extracellular molecule uptake in plasmonic laser perforation," *J. Biophotonics* published online (2013), 06/2013.

28. A. P. Rudhall et al., "Exploring the ultrashort pulse laser parameter space for membrane permeabilisation in mammalian cells," *Sci. Rep.* **2**, 858 (2012).
29. C. Yao et al., "Influence of laser parameters on nanoparticle-induced membrane permeabilization," *J. Biomed. Opt.* **14**(5), 054034 (2009).
30. V. Oberle et al., "Efficient transfer of chromosome-based DNA constructs into mammalian cells," *Biochim. Biophys. Acta.* **1676**(3), 223–230 (2004).
31. E. Eksioğlu-Demiralpa et al., "A method for functional evaluation of caspase activation pathways in intact lymphoid cells using electroporation-mediated protein delivery and flow cytometric analysis," *J. Immunol. Methods* **275**(1–2), 41–56 (2003).
32. R. Todorova, "Estimation of methods of protein delivery into mammalian cells—a comparative study by electroporation and bioporter assay," *Appl. Biochem. Microbiol.* **45**(4), 444–448 (2009).

Tatsuki Mitsuhashi received his BS degree in engineering from the Keio University in 2012. Currently, he is a graduate student in the School of Integrated Design Engineering, Keio University. His research interests include laser-based nanomedicine, laser-cell perforation, drug delivery, and minimally invasive laser therapeutic technology.

Mitsuhiro Terakawa received his BS, MS, and PhD degrees in engineering from Keio University in 2003, 2005, and 2007, respectively. In 2007, he joined the Wellman Center for Photomedicine, Massachusetts General Hospital, Harvard Medical School, as a research fellow. Currently, he is an assistant professor in the Department of Electronics and Electrical Engineering at Keio University. His research interests include laser processing, plasmonic nanofabrication, and minimally invasive laser therapeutic technology.